HSF1 Activation Can Restrict HIV Replication

Emmanuel E. Nekongo[1,†], Anna I. Ponomarenko[1,†], Mahender B. Dewal[1], Vincent L. Butty[2], Edward P. Browne[3], Matthew D. Shoulders[1*]

[1]Department of Chemistry, Massachusetts Institute of Technology, Cambridge, MA U.S.A. 02139
[2]BioMicro Center, Massachusetts Institute of Technology, Cambridge, MA U.S.A. 02139
[3]Department of Medicine, University of North Carolina School of Medicine, Chapel Hill, NC U.S.A. 27516

[†]These authors contributed equally to this work.

*To whom correspondence may be addressed:

Matthew D. Shoulders
Department of Chemistry
Massachusetts Institute of Technology
77 Massachusetts Avenue
Building 16, Room 573A
Cambridge, MA 02139
Phone: (617) 452-3525
Email: mshoulde@mit.edu

Host protein folding stress responses can play important roles in RNA virus replication and evolution. Prior work suggested a complicated interplay between the cytosolic proteostasis stress response, controlled by the transcriptional master regulator heat shock factor 1 (HSF1), and human immunodeficiency virus-1 (HIV-1). We sought to uncouple HSF1 transcription factor activity from cytotoxic proteostasis stress and thereby better elucidate the proposed role(s) of HSF1 in the HIV-1 lifecycle. To achieve this objective, we used chemical genetic, stress-independent control of HSF1 activity to establish whether and how HSF1 influences HIV-1 replication. Stress-independent HSF1 induction decreased both the total quantity and infectivity of HIV-1 virions. Moreover, HIV-1 was unable to escape HSF1-mediated restriction over the course of several serial passages. These results clarify the interplay between the host's heat shock response and HIV-1 infection and motivate continued investigation of chaperones as potential antiviral therapeutic targets.

Keywords

human immunodeficiency virus-1 (HIV-1), heat shock factor 1 (HSF1), heat shock response (HSR), cytosolic proteostasis, protein folding and assembly

Human immunodeficiency virus-1 (HIV-1) remains a serious global health threat, with approximately 37 million people currently living with HIV/AIDS.[1] While the number of HIV-related deaths continues to decline, owing to advances in treatment and prevention strategies in the past decades,[2] the epidemic still claims nearly one million lives annually. The problems of latent infection and drug resistance remain, as does the continued failure to develop an effective HIV vaccine.

With respect to the development of new therapeutic modalities impervious to antiviral resistance mechanisms, not just for HIV but also for other RNA viruses, the alternative strategy of targeting host systems instead of the rapidly mutating virus itself has gained increasing traction.[3-4] As a minimalistic pathogen, HIV-1 requires complex interactions with host systems for replication.[5-6] A clear understanding of the intimate interplay between the host and the virus is essential to provide an effective roadmap for viable, host-targeted antiviral therapeutics.[4, 7]

Stress responses evolved to defend cells against damaging internal and external stimuli. In some cases, stress responses can provide defenses against invading pathogens. However, numerous viral pathogens have also developed strategies to take advantage of these same host stress signaling pathways. A prominent example of the latter is the cellular heat shock response (HSR), which is responsible for maintaining proteostasis in the cytosol and nucleus.[8] The HSR is controlled by its master regulator, the heat shock factor 1 (HSF1) transcription factor. High levels of HSF1 activity can be triggered by a variety of stressors, including protein misfolding in the cytosol. HSF1-mediated upregulation of numerous heat shock protein (HSP) chaperones and quality control proteins serves to restore proteostasis, after which HSF1 activity is reduced to basal levels.[9] Many host chaperones, including HSP70 and HSP90, are hijacked by diverse viruses to assist viral protein folding and thereby enable virion production.[10-13] Inhibition of these same chaperones can suppress viral replication.[14-18] Moreover, chaperones can potentiate the evolution of viral proteins. Changes in cellular proteostasis capacity can modulate viral evolutionary trajectories,[19-21] and even define the accessibility of destabilized viral protein variants that can enable innate immune system escape.[22]

Hence, host HSF1 activity and the functions of HSF1-regulated host chaperones are often beneficial for viruses.[10-13, 19-21] However, this conclusion derives largely from studies on just a few viruses, including influenza, Dengue, Zika, and polio – with limited studies on retroviruses. Similar phenomena might be expected for retroviruses, which also have high mutation rates and a need to fold their proteins. On the other hand, the requirement for host genome integration in particular adds an additional step that could be differentially influenced by HSF1 and other HSPs.

Prior work has suggested an intimate role for the host cell's HSR in multiple steps of the HIV-1 lifecycle. The complexity of HSF1 engagement during HIV-1 replication is perhaps best illustrated by HSF1's apparent ability to either assist[12, 23-26] or restrict[27-28] HIV-1 propagation depending on the method used to perturb

HSF1 activity. For example, heat stress stimulates HIV-1 gene transcription[23] and viral replication.[25-26] In other work, transient overexpression of wild-type HSF1 assisted HIV-1 generation[24] and reactivation from latency,[12] while HSF1 knockdown proved deleterious for HIV-1 production. Alternatively, transient overexpression of a constitutively active variant of HSF1 suppressed long terminal repeat (LTR)-driven viral transcription[27] and downregulated HIV-induced inflammation.[28] Similarly, the reported roles of individual HSF1-controlled chaperones in HIV-1 replication extensively vary between different experimental systems.[29-36] In sum, although the details are still unclear, there is clearly a complicated interplay between the host's HSR and the HIV-1 lifecycle.

Our objective was to isolate the direct effects of HSF1 activation from the indirect effects of the cellular stressors that are traditionally used to activate HSF1, thereby gaining a clear understanding of the consequences of HSF1 activity for HIV-1 replication. The achievement of this goal requires a tool for stress-independent HSF1 activation. Heat induction of HSF1 activity is unsuitable because heat is a pleiotropic stress that causes acute and severe protein misfolding throughout the proteome. Genetic methods are preferred as they avoid HSR activation, however the extent of HSF1 activation is limited by cellular compensation mechanisms. For example, overexpression of wild-type HSF1 increases the protein levels of the transcription factor, but the excess HSF1 protein is subject to chaperone-mediated regulation and is thus kept in an inactive state.[37] Genetic HSF1 knockdown is also inefficient, owing to compensating proteostasis mechanisms.[38] Finally, unregulated overexpression of constitutively active HSF1 variants must be employed with great caution to avoid nonphysiologic levels of HSF1 induction and consequent pleiotropic remodeling of the transcriptome.[39] Chemical methods for directly regulating HSF1 activity are preferred.[40-42]

We first sought to generate a system in which stress-independent, small molecule-mediated induction of HSF1 activity was possible. We engineered a stable, single-colony human T lymphocyte (CEM) cell line in which the expression of a constitutively active variant of HSF1 (cHSF1)[39, 43] was placed under control of the doxycycline (dox)-dependent tetracycline (tet) repressor.[39] Treatment of the resulting CEM^{cHSF1} cell line (Figure 1A) with dox resulted in the expression of HSF1 target genes, as demonstrated by the increased transcript levels of HSP90, HSP70, and HSP40 (Figure 1B). The single colony cell line was carefully chosen to ensure that the upregulation of these downstream chaperones was similar in magnitude to that caused by HSF1 activation by the prototypical chemical stressor As(III)[44] (Figure 1B), ensuring that HSF1 activity was not induced beyond physiologically accessible levels.[39] We also generated a fluorescent control cell line (CEM^{Ctrl}) in which cyan fluorescent protein (CFP) expression was similarly placed under control of the tet repressor.

With CEM^{cHSF1} and CEM^{Ctrl} cell lines in hand, we next sought to test whether stress-independent HSF1 activation impacted HIV-1 replication. We began by treating CEM^{cHSF1} and CEM^{Ctrl} cells with dox for 18 h to activate cHSF1 or CFP expression, respectively. Next, we infected these preactivated cells with NL4-3 HIV-1

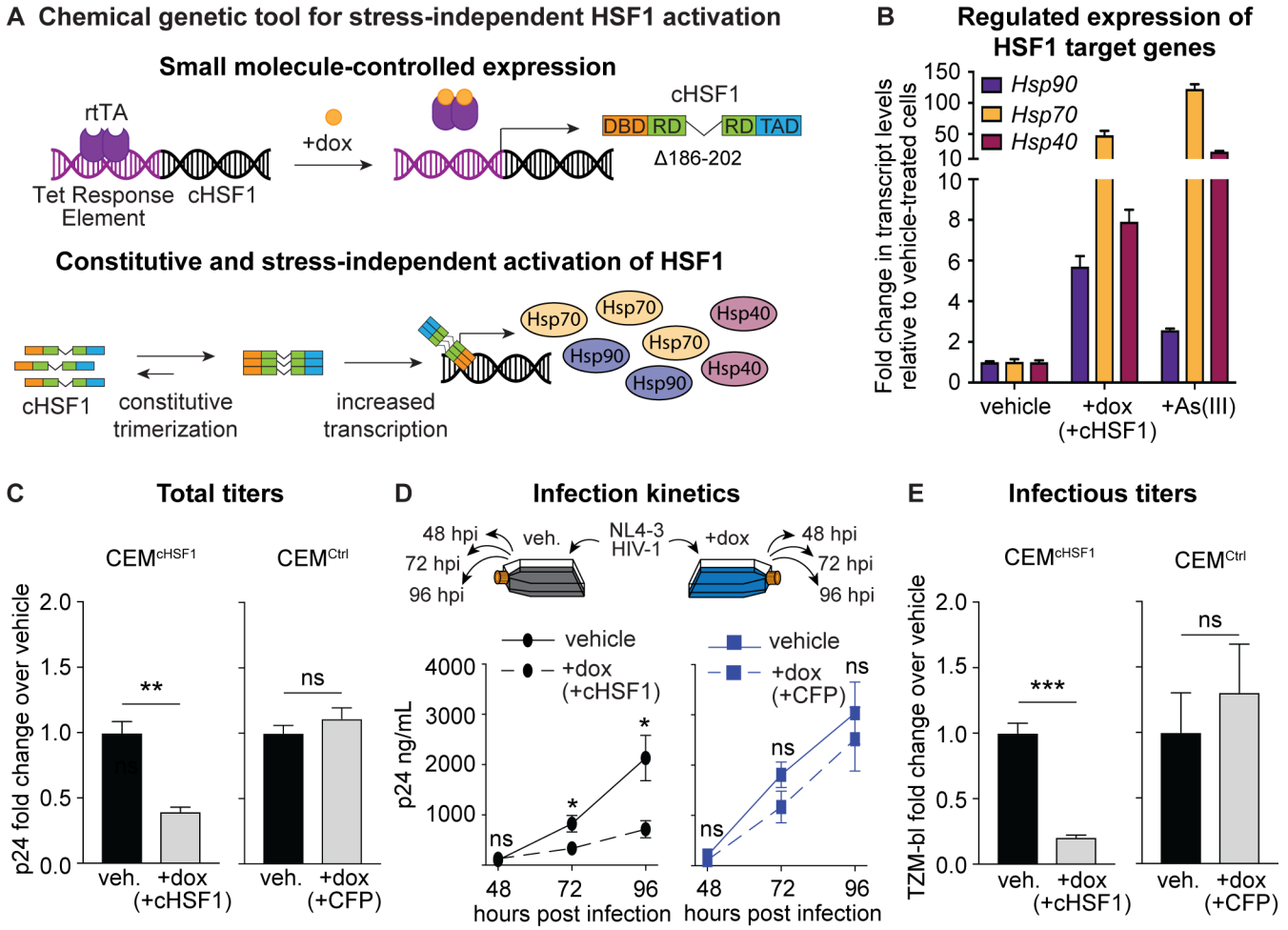

Figure 1. Stress-independent cHSF1 activation decreases HIV-1 replication and the infectivity of produced virions. (**A**) Chemical genetic tool for stress-independent, small molecule-regulated activation of HSF1. Treatment of CEM-^{cHSF1} cells with dox induces expression of cHSF1, which constitutively trimerizes and upregulates the expression of HSF1 target genes in the absence of acute proteostatic stress. (**B**) qPCR analysis of Hsp90 (*HSP90AA1*), Hsp70 (*HSPA1A*), and Hsp40 (*DNAJB1*) expression in CEM^{cHSF1} after 18 h of treatment with 1 µg/mL dox or 2 h of treatment with 100 µM sodium arsenite as a positive heat shock control. (**C**) Fold-change in p24 titers after 96 h of HIV-1 infection at an MOI of 0.04 in CEM^{cHSF1} and CEM^{Ctrl} cells, treated with 1 µg/mL dox, relative to vehicle-treated cells. (**D**) Schematic of a timecourse infection and total p24 viral titers during different infection time points in CEM^{cHSF1} and CEM^{Ctrl} cells. (**E**) Fold-change in infectious TZM-bl titers after 96 h of HIV-1 propagation in CEM^{cHSF1} and CEM^{Ctrl} cells, treated with 1 µg/mL dox, relative to vehicle-treated cells. *, **, ***, and ns correspond to *p*-values <0.05, <0.001, <0.0001, and not significant, respectively.

at a multiplicity of infection (MOI) of 0.04 for 96 h, followed by harvesting the infectious supernatant and titering using a p24 enzyme-linked immunosorbent assay (ELISA).

We observed that cHSF1 activation significantly reduced total p24 viral titers relative to cells with basal HSF1 activity (Figure 1C). In contrast, dox-induced expression of CFP in the CEM^{Ctrl} cell line did not alter p24 titers, showing that the result was attributable to cHSF1 activity and not to dox treatment. We further assessed infection kinetics by harvesting the viral supernatant at successive time points and titering using the p24 assay. The relative difference in p24 titers between cHSF1-activated versus vehicle-treated CEM^{cHSF1} cells became more pronounced as the infection progressed, with no significant difference observed in dox- versus vehicle-

treated CEM^{Ctrl} cells at any time point (Figure 1D). Finally, we used the TZM-bl assay[45] to quantify the infectious titers of collected viral supernatants. Successful infection of reporter TZM-bl cells activates the expression of β-galactosidase in an HIV-1 Tat-dependent manner, turning reporter cells blue in the presence of a 5-bromo-4-chloro-3-indolyl-*p*-D-galactopyranoside (X-Gal) chromogenic substrate. The fraction of stained cells is then proportional to the number of infectious viral particles.[45] We observed that, as also occurred with the p24 titers, infectious titers were indeed decreased by cHSF1 activation in CEM^{cHSF1} cells, whereas they did not change upon CFP activation in CEM^{Ctrl} cells (Figure 1E).

The high mutation rate of HIV-1 often promotes rapid escape from inhibitory pressure. Therefore, we next asked whether continuous propagation of HIV-1 under pressure from cHSF1 activity would result in rapid antiviral escape. We performed three serial passages in cHSF1-activated versus vehicle-treated CEM-^{cHSF1} cells (Figure 2A). At each passage, the pre-activated cells were infected at an MOI of 0.04 for 96 h, followed by harvesting the viral supernatant and titering. The infectious (TZM-bl) titers were used to initiate the subsequent passage at the same MOI. Notably, both total and infectious viral titers were still decreased in +cHSF1 cells relative to vehicle-treated cells even after the third serial passage (Figures 2B and 2C), indicating that the virus cannot readily adapt to cHSF1-mediated replication restriction.

One potential trivial explanation for HSF1's effect on HIV-1 replication could be cytotoxicity. We assessed cell health in the conditions of our viral propagation experiments by using a CellTiter-Glo assay. We observed that cellular ATP levels were not significantly altered by stress-independent cHSF1 activation (Figure 3A).

We next asked whether the observed inhibition of HIV-1 was specific to the HSR or could be replicated by stress-independent activation of other protein misfolding stress responses. We engineered a stable cell line, termed CEM^{DAX}, in which the IRE1-XBP1s and ATF6 arms of the unfolded protein response (UPR), which is responsible for maintaining proteostasis in the secretory

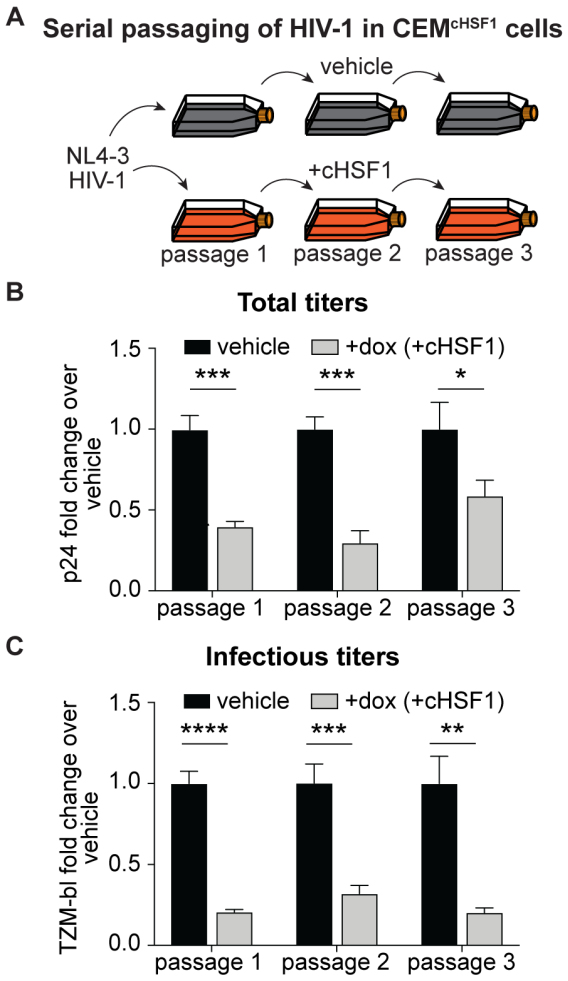

Figure 2. HIV-1 does not adapt to escape HSF1 activation over the course of three serial passages. (**A**) Schematic of NL4-3 HIV-1 serial passaging. CEM^{cHSF1} cells were pretreated with 1 μg/mL dox for 18 h prior to infection with NL4-3 HIV-1 for 96 h at an MOI of 0.04. Infectious titers of the viral supernatant were determined using the TZM-bl assay, and then, the supernatant was used to infect the subsequent passage at the same MOI. (**B**) Fold-change in total p24 and (**C**) infectious TZM-bl titers at each passage. *, **, ***, and **** correspond to *p*-values < 0.05, < 0.01, < 0.001, and < 0.0001, respectively.

pathway,[46] could be activated by small molecules in a stress-independent manner. Our approach was to render XBP1s expression dox-inducible by placing the *XBP1s* gene under control of the tetracycline promoter.[47] To control the ATF6 arm of the UPR, we fused the transcriptionally active form of ATF6 to an *Escherichia coli* dihydrofolate reductase (DHFR) destabilized domain.[48] Treatment of CEM^{DAX} cells with trimethoprim (TMP) stabilizes the DHFR domain, resulting in ATF6 transcriptional activity. This strategy is well-established for stress-independent control of the IRE1-XBP1s and ATF6 arms of the unfolded protein response.[21, 41, 49-54] We verified the selective, dox-dependent induction of XBP1s target genes and the selective, TMP-dependent induction of ATF6 target genes in CEM^{DAX} cells using qPCR (Figure S1).[49] We also employed a fluorescent control CEM^{Ctrl} cell line stably engineered to express dox-inducible CFP and *E. coli* DHFR-fused yellow fluorescent protein (YFP). We then pretreated CEM^{DAX} and CEM^{Ctrl} cells with dox and TMP for 18 h to activate the corresponding constructs, infected the cells with HIV-1 at an MOI of 0.04, and measured the resulting p24 titers after 96 h. No significant change in p24 titers was observed upon dox and TMP treatment in either the CEM^{DAX} or the CEM^{Ctrl} cells (Figure 3B). Thus, HSF1-mediated abrogation of HIV-1 replication is a specific feature of HSR activation, not a general consequence of inducing protein misfolding stress responses.

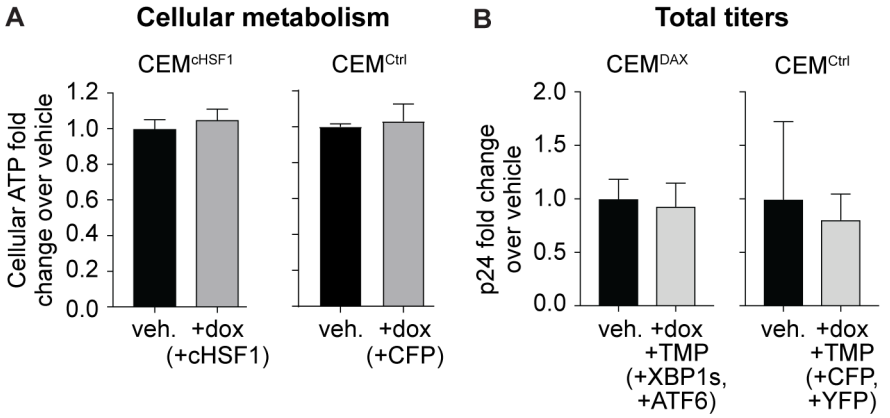

Figure 3. Decreased HIV-1 replication is not attributable to HSF1-induced cytotoxicity. (**A**) Cellular ATP levels upon 1 μg/mL dox treatment of CEM^{cHSF1} and CEM^{Ctrl} cells for 96 h, as assessed using a CellTiter-Glo assay. (**B**) Total p24 viral titers upon 1 μg/mL dox and 10 μM TMP treatment of CEM^{DAX} and CEM^{Ctrl} cell lines.

Next, we used RNA-Seq to globally assess transcriptome remodeling owing to cHSF1 activation in CEM^{cHSF1} cells. In particular, we were interested in whether or not stress-independent cHSF1 induction might elicit an antiviral response in CEM^{cHSF1} cells. As expected, given the specificity of our stress-independent, chemical induction of cHSF1, the most prominent upregulated genes were all well-known components of the HSR (Figures 4 and S2, Table S1).[39] Also, as expected, no significant induction of UPR target genes was observed (Figure 4 and Table S1).

We applied gene set enrichment analysis (GSEA)[55] (Table S2) to better understand key features of the transcriptome remodeling caused by cHSF1

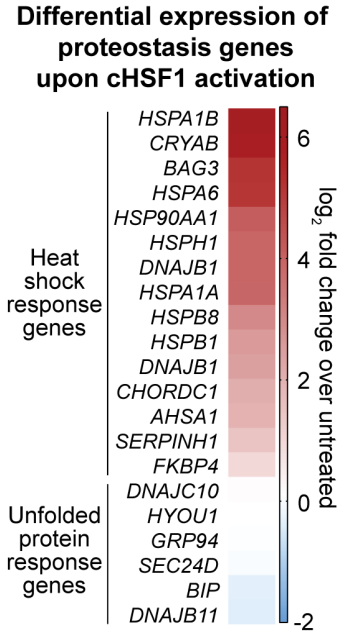

Figure 4. Heat map showing the differential expression of select proteostasis genes upon stress-independent cHSF1 activation with 1 μg/mL dox for 18 h in CEM^{cHSF1} cells relative to vehicle treatment.

activation. We observed that known HSR-related gene sets were massively enriched (MSigDB c5 collection; Figure 5A and Tables S2A and S2B). Furthermore, the HSF1-binding motif itself was strongly enriched upstream of genes that were found to be responsive to stress-independent cHSF1 activation (MSigDB c3 collection, Figure S3 and Table S2C). However, we did not observe any significant enrichment of antiviral restriction factors using the MSigDB c5 collection (see Figure 5B for example enrichment plots and Tables S2A and S2B). Similarly, when other functional databases regrouped in the MSigDB c2 collections were interrogated, viral- and interferon-response pathways tended either not to display any bias or even to be enriched among downregulated gene sets (Tables S2D and S2E).

These observations suggest that stress-independent HSF1 activation in CEM^{cHSF1} cells does not inhibit HIV-1 replication by inducing a general antiviral response. We next examined individual genes within the broad

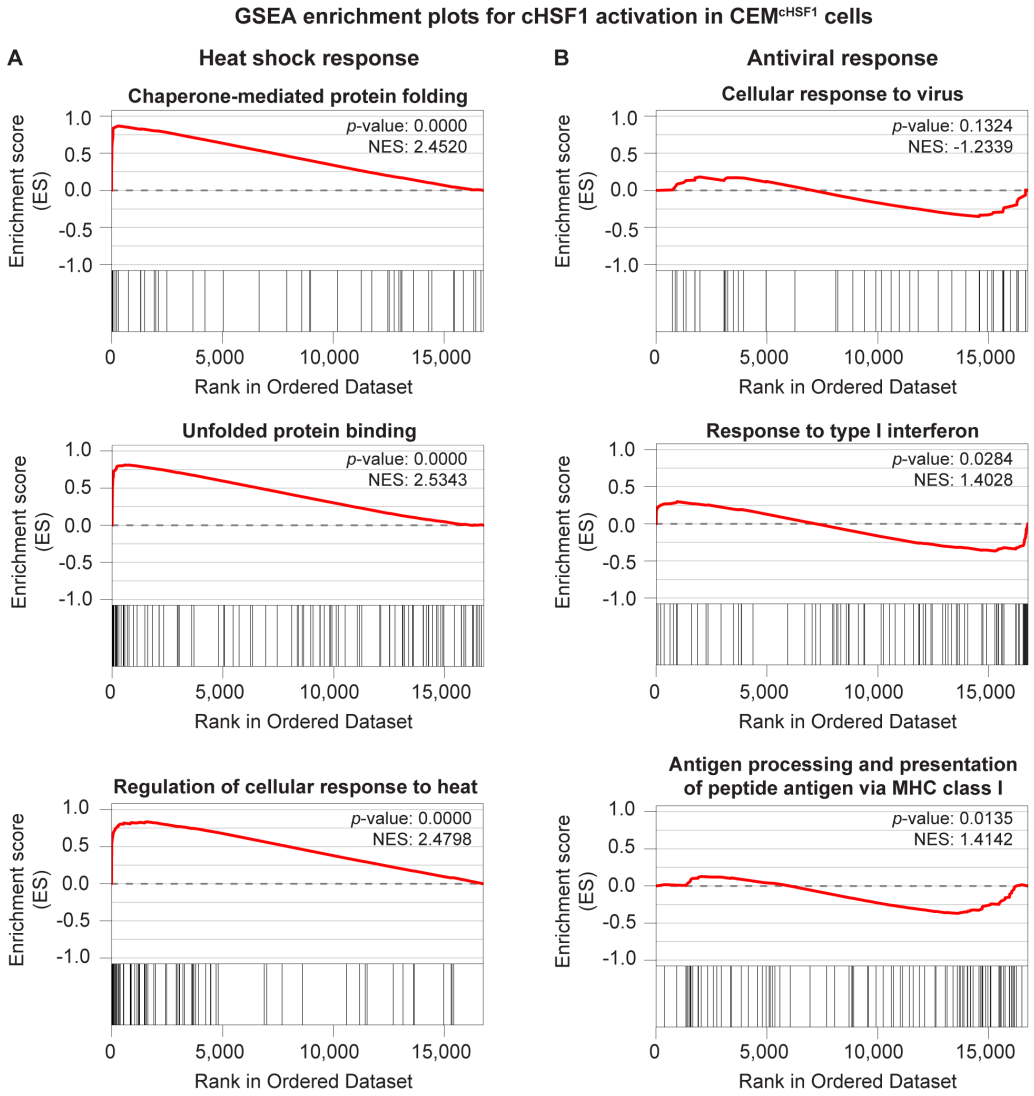

Figure 5. Stress-independent HSF1 induction activates heat shock response genes and does not trigger a broad-scale antiviral response. **(A)** Selected gene set enrichment plots for heat shock response-related and (**B**) antiviral response-related gene sets in CEM^{cHSF1} cells treated with 1 µg/mL doxycycline for 18 h to induce cHSF1. These enrichment plots are drawn from the MSigDB c5 collection. See Table S2 for the complete gene set enrichment analysis.

gene ontology group "Defense Response to Virus" (Table S3). While typical components of the general antiviral defense response, including many interferon-related genes, were not enriched or even downregulated, we were intrigued to note that the most upregulated gene in the entire gene set was *ZC3HAV1*. *ZC3HAV1* encodes the zinc finger antiviral protein ZAP (also known as PARP13), and was upregulated 3.2-fold in our RNA-Seq experiment upon cHSF1 induction. ZAP is known to restrict the replication of multiple viruses, particularly including HIV-1,[56-57] by targeting viral mRNA in the cytoplasm for degradation.[58] ZAP can also bind HSF1[59] and assist HSF1 binding to DNA prior to heat shock.[60] Indeed, the first intron of ZAP possesses an HSF1-binding motif, located in a putative chromatin regulatory region denoted by a peak of H3K27-acetylated histones, as reported by the Encyclopedia of DNA Elements (ENCODE) consortium in an immortalized B-cell line (chromatin immunoprecipitation (ChIP)-Seq ENCODE track on the UCSC Genome Browser).[61] We used qPCR to confirm that the induction of cHSF1 in CEM^{cHSF1} cells indeed triggered upregulation of ZAP mRNA (Figure S4). On the basis of these observations, ZAP induction is likely to contribute to cHSF1-mediated inhibition of HIV-1 replication.

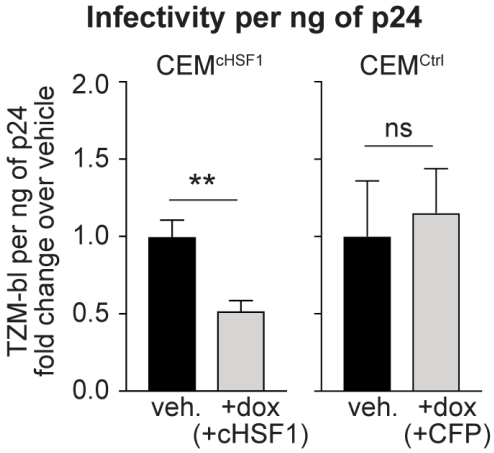

Figure 6. HSF1 reduces infectivity of newly produced virions. Fold-change in infectious TZM-bl titers per ng of p24 after 96 h of HIV-1 infection at an MOI of 0.04 in CEM^{cHSF1} and CEM^{Ctrl} cells treated with 1 μg/mL dox, relative to vehicle-treated cells. ** and ns correspond to p-values < 0.01 and not significant, respectively.

Although ZAP induction may play a role in the inhibition of HIV-1 replication, the key finding from our RNA-Seq analysis was that cHSF1 activation largely drives a transcriptional remodeling of the cellular chaperone network, with minimal impacts on immune responses and traditional viral restriction factors. A number of these chaperones have been implicated in the HIV lifecycle and play important roles in viral protein folding and assembly.[62-64] Thus, it is possible that the remodeled cytosolic and nuclear proteostasis network, which did not evolve to support HIV-1 replication but rather to ensure cellular proteostasis, might disrupt these steps in the lifecycle by diverting viral proteins from function or the orchestrated virion assembly process. In this regard, it is noteworthy that comparing the total (p24) to the infectious (TZM-bl) viral titers, we observed that the fraction of produced virions that are infection-competent significantly decreased upon cHSF1 activation (Figure 6). This observation is consistent with cHSF1 activation disrupting steps in the viral lifecycle such as viral protein folding and/or virion assembly that could lead to the production of a larger fraction of defective viral particles. Because host chaperones not only directly modulate viral protein folding and assembly but also participate in earlier steps of the viral replication cycle, such as nuclear import,[34] genome integration,[65] and transcription,[33, 36] we do not exclude the possibility of additional inhibitory roles of the cHSF1-remodeled proteostasis network in these processes.

In summary, the use of a chemically controlled cHSF1 construct allowed us to investigate the direct consequences of HSF1 activation at physiologically relevant levels, eliminating the requirement for inducing global protein misfolding while also avoiding the off-target consequences of cHSF1 overexpression. We were also able to avoid the complications associated with transient overexpression of HSF1 or cHSF1,[39, 42] including off-target gene induction, which convoluted prior studies. Using this approach, we demonstrated that stress-independent HSF1 activation restricts HIV-1 replication in CEM cells. When cHSF1 was activated, fewer total HIV-1 virions were produced and the proportion of infectious virions was also lowered. Moreover, cHSF1-mediated inhibition of HIV-1 replication persisted through three consecutive serial passages without detectable recovery of viral titers, suggesting that escape mechanisms are not readily available to the virus. The effects of cHSF1 activation were HSR-specific and not attributable to reductions in host cell health, off-target cHSF1 activity, or activation of protein misfolding stress responses in general.

The exact molecular mechanisms of HSF1-mediated restriction of HIV-1 replication remain an important subject for further study and are likely multifactorial. First, viral transcripts are known to be targeted to degradation by the HSF1-controlled host restriction factor ZAP, which has an HSF1-binding promoter and was transcriptionally upregulated in our system despite the absence of a general antiviral response induced by cHSF1. Second, cHSF1 activation reduces the infectivity of newly formed virions. This observation suggests that the remodeled host chaperone network promotes the formation of defective viral particles. While deciphering the origins of HSF1-mediated inhibition of HIV-1 replication and elucidating *in vivo* relevance of these findings requires future investigation, this work clearly implicates HSF1 as a host antiviral restriction factor for HIV-1 and motivates continued consideration of host HSR-targeted therapeutics to address retroviral infections.

Methods

Detailed protocols for the following procedures can be found in the Supporting Information: stable cell line construction, quantitative RT-PCR, HIV-1 infection, p24 assays, TZM-bl assays, CellTiter-Glo viability assays, RNA-Seq, GSEA, and statistical analyses.

Supporting Information

The Supporting Information is available free of charge at https://pubs.acs.org/doi/10.1021/acsinfecdis.0c00166 .

Complete experimental methods; selective induction of XBP1s and/or ATF6 target genes in CEMDAX cells; transcriptional profile of the HSF1-activated host environment; heat shock factor motif enrichment upon cHSF1 induction; induction of cHSF1 activating ZAP transcription; sequences of RT-PCR primers used (PDF)

RNA-Seq characterization of CEMcHSF1 cells: Differential expression analysis of the HSF1-activated environment (XLSX)

RNA-Seq characterization of CEMcHSF1 cells: Gene set enrichment analysis (XLSX)

Gene list for the "Defense Response to Virus" gene ontology group (XLSX)

Present/Current Author Addresses

E.E.N. current address: Ultragenyx Gene Therapy, 150 Presidential Way, Woburn, MA 01801, USA.

M.B.D. current address: Expansion Technologies, Inc., 1 Kendall Sq., Cambridge, MA 02139, USA.

Corresponding Author Information

Matthew D. Shoulders: mshoulde@mit.edu

Author Contributions

E.E.N. and M.D.S. conceived the project. E.E.N., A.I.P., M.B.D., E.P.B., and M.D.S. designed the experiments. E.E.N., A.I.P., and M.B.D. performed the experiments. E.E.N., A.I.P., V.L.B., E.P.B., and M.D.S. analyzed the data. M.D.S. supervised the research. A.I.P. drafted the manuscript. All authors edited and approved the manuscript.

The authors declare no competing financial interest.

Acknowledgements

This work was supported by the Smith Family Foundation Award for Excellence in Biomedical Research, the National Science Foundation (CAREER Award 1652390), the National Institutes of Health (Grants 1DP2GM119162 and 1R35GM136354) to M.D.S., the MIT Center for Environmental Health Sciences (P30-ES002109), and the Koch Institute (P30-CA14051). E.E.N. was supported by a UNCF-Merck Postdoctoral Fellowship.

References

1. World Health Organization (accessed June 3, 2019) Summary of the global HIV epidemic (2017), https://www.who.int/hiv/data/2017_summary-global-hiv-epidemic.png?ua=1.
2. Cihlar, T.; Fordyce, M., Current status and prospects of HIV treatment. *Curr. Opin. Virol.* **2016,** *18*, 50-56.
3. Jean, M. J.; Fiches, G.; Hayashi, T.; Zhu, J., Current strategies for elimination of HIV-1 latent reservoirs using chemical compounds targeting host and viral factors. *AIDS Res. Hum. Retroviruses* **2019,** *35*, 1-24.
4. Park, R. J.; Wang, T.; Koundakjian, D.; Hultquist, J. F.; Lamothe-Molina, P.; Monel, B.; Schumann, K.; Yu, H.; Krupzcak, K. M.; Garcia-Beltran, W. et al. A genome-wide CRISPR screen identifies a restricted set of HIV host dependency factors. *Nat. Genet.* **2017,** *49*, 193-203.
5. Brass, A. L.; Dykxhoorn, D. M.; Benita, Y.; Yan, N.; Engelman, A.; Xavier, R. J.; Lieberman, J.; Elledge, S. J., Identification of host proteins required for HIV infection through a functional genomic screen. *Science* **2008,** *319*, 921-926.
6. Jäger, S.; Cimermancic, P.; Gulbahce, N.; Johnson, J. R.; McGovern, K. E.; Clarke, S. C.; Shales, M.; Mercenne, G.; Pache, L.; Li, K. et al. Global landscape of HIV–human protein complexes. *Nature* **2012,** *481*, 365.
7. Arhel, N.; Kirchhoff, F., Host proteins involved in HIV infection: new therapeutic targets. *Biochim. Biophys. Acta, Mol. Basis Dis.* **2010,** *1802*, 313-321.
8. Aviner, R.; Frydman, J., Proteostasis in viral infection: unfolding the complex virus–chaperone interplay. *Cold Spring Harbor Perspect. Biol.* **2019**, a034090.
9. Richter, K.; Haslbeck, M.; Buchner, J., The heat shock response: life on the verge of death. *Mol. Cell* **2010,** *40*, 253-266.
10. Filone, C. M.; Caballero, I. S.; Dower, K.; Mendillo, M. L.; Cowley, G. S.; Santagata, S.; Rozelle, D. K.; Yen, J.; Rubins, K. H.; Hacohen, N. et al. The master regulator of the cellular stress response (HSF1) is critical for orthopoxvirus infection. *PLoS Pathog.* **2014,** *10*, e1003904.
11. Tsai, T.-T.; Chen, C.-L.; Tsai, C.-C.; Lin, C.-F., Targeting heat shock factor 1 as an antiviral strategy against dengue virus replication in vitro and in vivo. *Antiviral Res.* **2017,** *145*, 44-53.
12. Pan, X.-Y.; Zhao, W.; Zeng, X.-Y.; Lin, J.; Li, M.-M.; Shen, X.-T.; Liu, S.-W., Heat shock factor 1 mediates latent HIV reactivation. *Sci. Rep.* **2016,** *6*, 26294.
13. Wang, F.-W.; Wu, X.-R.; Liu, W.-J.; Liao, Y.-J.; Lin, S.; Zong, Y.-S.; Zeng, M.-S.; Zeng, Y.-X.; Mai, S.-J.; Xie, D., Heat shock factor 1 upregulates transcription of Epstein–Barr Virus nuclear antigen 1 by binding to a heat shock element within the BamHI-Q promoter. *Virology* **2011,** *421*, 184-191.
14. Geller, R.; Taguwa, S.; Frydman, J., Broad action of Hsp90 as a host chaperone required for viral replication. *Biochim. Biophys. Acta, Mol. Cell Res.* **2012,** *1823*, 698-706.
15. Joshi, P.; Sloan, B.; Torbett, B. E.; Stoddart, C. A., Heat shock protein 90AB1 and hyperthermia rescue infectivity of HIV with defective cores. *Virology* **2013,** *436*, 162-172.
16. Heaton, N. S.; Moshkina, N.; Fenouil, R.; Gardner, T. J.; Aguirre, S.; Shah, P. S.; Zhao, N.; Manganaro, L.; Hultquist, J. F.; Noel, J. et al. Targeting viral proteostasis limits influenza virus, HIV, and dengue virus infection. *Immunity* **2016,** *44*, 46-58.
17. Taguwa, S.; Maringer, K.; Li, X.; Bernal-Rubio, D.; Rauch, J. N.; Gestwicki, J. E.; Andino, R.; Fernandez-Sesma, A.; Frydman, J., Defining Hsp70 subnetworks in dengue virus replication reveals key vulnerability in flavivirus infection. *Cell* **2015,** *163*, 1108-1123.
18. Taguwa, S.; Yeh, M.-T.; Rainbolt, T. K.; Nayak, A.; Shao, H.; Gestwicki, J. E.; Andino, R.; Frydman, J., Zika virus dependence on host Hsp70 provides a protective strategy against infection and disease. *Cell Rep.* **2019,** *26*, 906-920. e3.
19. Phillips, A. M.; Gonzalez, L. O.; Nekongo, E. E.; Ponomarenko, A. I.; McHugh, S. M.; Butty, V. L.; Levine, S. S.; Lin, Y.-S.; Mirny, L. A.; Shoulders, M. D., Host proteostasis modulates influenza evolution. *eLife* **2017,** *6*, e28652.

20. Geller, R.; Pechmann, S.; Acevedo, A.; Andino, R.; Frydman, J., Hsp90 shapes protein and RNA evolution to balance trade-offs between protein stability and aggregation. *Nat. Commun.* **2018,** *9*, 1781.
21. Phillips, A. M.; Doud, M. B.; Gonzalez, L. O.; Butty, V. L.; Lin, Y.-S.; Bloom, J. D.; Shoulders, M. D., Enhanced ER proteostasis and temperature differentially impact the mutational tolerance of influenza hemagglutinin. *eLife* **2018,** *7* e38795.
22. Phillips, A. M.; Ponomarenko, A. I.; Chen, K.; Ashenberg, O.; Miao, J.; McHugh, S. M.; Butty, V. L.; Whittaker, C. A.; Moore, C. L.; Bloom, J. D. et al. Destabilized adaptive influenza variants critical for innate immune system escape are potentiated by host chaperones. *PLoS Biol.* **2018,** *16*, e3000008.
23. Kretz-Remy, C.; Munsch, B.; Arrigo, A.-P., NFκB-dependent transcriptional activation during heat shock recovery. Thermolability of the NFκB.IκB complex. *J. Biol. Chem.* **2001,** *276*, 43723-43733.
24. Rawat, P.; Mitra, D., Cellular heat shock factor 1 positively regulates human immunodeficiency virus-1 gene expression and replication by two distinct pathways. *Nucleic Acids Res.* **2011,** *39*, 5879-5892.
25. Roesch, F.; Meziane, O.; Kula, A.; Nisole, S.; Porrot, F.; Anderson, I.; Mammano, F.; Fassati, A.; Marcello, A.; Benkirane, M. et al. Hyperthermia stimulates HIV-1 replication. *PLoS Pathog.* **2012,** *8*, e1002792.
26. Hashimoto, K.; Baba, M.; Gohnai, K.; Sato, M.; Shigeta, S., Heat shock induces HIV-1 replication in chronically infected promyelocyte cell line OM10.1. *Arch. Virol.* **1996,** *141*, 439-447.
27. Ignatenko, N. A.; Gerner, E. W., Regulation of the HIV1 long terminal repeat by mutant heat shock factor. *Exp. Cell Res.* **2003,** *288*, 1-8.
28. Pan, X.; Lin, J.; Zeng, X.; Li, W.; Wu, W.; Lu, W. Z.; Liu, J.; Liu, S., Heat shock factor 1 suppresses the HIV-induced inflammatory response by inhibiting nuclear factor-κB. *Cell. Immunol.* **2018,** *327*, 26-35.
29. Vozzolo, L.; Loh, B.; Gane, P. J.; Tribak, M.; Zhou, L.; Anderson, I.; Nyakatura, E.; Jenner, R. G.; Selwood, D.; Fassati, A. Gyrase B inhibitor impairs HIV-1 replication by targeting HSP90 and the capsid protein. *J. Biol. Chem.* **2010**, 285, 39314-28.
30. Anderson, I.; Low, J. S.; Weston, S.; Weinberger, M.; Zhyvoloup, A.; Labokha, A. A.; Corazza, G.; Kitson, R. A.; Moody, C. J.; Marcello, A. et al. Heat shock protein 90 controls HIV-1 reactivation from latency. *Proc. Natl. Acad. Sci. U. S. A.* **2014,** *111*, E1528-E1537.
31. Urano, E.; Morikawa, Y.; Komano, J., Novel role of HSP40/DNAJ in the regulation of HIV-1 replication. *JAIDS, J. Acquir. Immune Defic. Syndr.* **2013,** *64*, 154-162.
32. Kumar, M.; Mitra, D., Heat shock protein 40 is necessary for human immunodeficiency virus-1 Nef-mediated enhancement of viral gene expression and replication. *J. Biol. Chem.* **2005,** *280*, 40041-50.
33. Kumar, M.; Rawat, P.; Khan, S. Z.; Dhamija, N.; Chaudhary, P.; Ravi, D. S.; Mitra, D., Reciprocal regulation of human immunodeficiency virus-1 gene expression and replication by heat shock proteins 40 and 70. *J. Mol. Biol.* **2011,** *410*, 944-958.
34. Agostini, I.; Popov, S.; Li, J.; Dubrovsky, L.; Hao, T.; Bukrinsky, M., Heat-shock protein 70 can replace viral protein R of HIV-1 during nuclear import of the viral preintegration complex. *Exp. Cell Res.* **2000,** *259*, 398-403.
35. Iordanskiy, S.; Zhao, Y.; DiMarzio, P.; Agostini, I.; Dubrovsky, L.; Bukrinsky, M., Heat-shock protein 70 exerts opposing effects on Vpr-dependent and Vpr-independent HIV-1 replication in macrophages. *Blood* **2004,** *104*, 1867-1872.
36. Chaudhary, P.; Khan, S. Z.; Rawat, P.; Augustine, T.; Raynes, D. A.; Guerriero, V.; Mitra, D., Hsp70 binding protein 1 (HspBP1) suppresses HIV-1 replication by inhibiting NF-κB mediated activation of viral gene expression. *Nucleic Acids Res.* **2016,** *44*, 1613-1629.
37. Zuo, J.; Baler, R.; Dahl, G.; Voellmy, R., Activation of the DNA-binding ability of human heat shock transcription factor 1 may involve the transition from an intramolecular to an intermolecular triple-stranded coiled-coil structure. *Mol. Cell. Biol.* **1994,** *14*, 7557-7568.
38. Mahat, D. B.; Salamanca, H. H.; Duarte, F. M.; Danko, C. G.; Lis, J. T., Mammalian heat shock response and mechanisms underlying its genome-wide transcriptional regulation. *Mol. Cell* **2016,** *62*, 63-78.

39. Ryno, L. M.; Genereux, J. C.; Naito, T.; Morimoto, R. I.; Powers, E. T.; Shoulders, M. D.; Wiseman, R. L., Characterizing the altered cellular proteome induced by the stress-independent activation of heat shock factor 1. *ACS Chem. Biol.* **2014,** *9*, 1273-1283.
40. Moore, C. L.; Dewal, M. B.; Nekongo, E. E.; Santiago, S.; Lu, N. B.; Levine, S. S.; Shoulders, M. D., Transportable, chemical genetic methodology for the small molecule-mediated inhibition of heat shock factor 1. *ACS Chem. Biol.* **2016,** *11*, 200-10.
41. Shoulders, M. D.; Ryno, L. M.; Cooley, C. B.; Kelly, J. W.; Wiseman, R. L., Broadly applicable methodology for the rapid and dosable small molecule-mediated regulation of transcription factors in human cells. *J. Am. Chem. Soc.* **2013,** *135*, 8129-32.
42. Sebastian, R. M.; Shoulders, M. D., Chemical biology framework to illuminate proteostasis. *Annu. Rev. Biochem.* **2020,** *89*, in press.
43. Voellmy, R., Dominant-positive and dominant-negative heat shock factors. *Methods* **2005,** *35*, 199-207.
44. Del Razo, L. M.; Quintanilla-Vega, B.; Brambila-Colombres, E.; Calderón-Aranda, E. S.; Manno, M.; Albores, A., Stress proteins induced by arsenic. *Toxicol. Appl. Pharmacol.* **2001,** *177*, 132-148.
45. Kimpton, J.; Emerman, M., Detection of replication-competent and pseudotyped human immunodeficiency virus with a sensitive cell line on the basis of activation of an integrated beta-galactosidase gene. *J. Virol.* **1992,** *66*, 2232-2239.
46. Wong, M. Y.; DiChiara, A. S.; Suen, P. H.; Chen, K.; Doan, N.-D.; Shoulders, M. D., Adapting secretory proteostasis and function through the unfolded protein response. *Curr. Top. Microbiol. Immunol.* **2017,** *414*, 1-25.
47. Lee, A.-H.; Iwakoshi, N. N.; Glimcher, L. H., XBP-1 regulates a subset of endoplasmic reticulum resident chaperone genes in the unfolded protein response. *Mol. Cell. Biol.* **2003,** *23*, 7448-59.
48. Iwamoto, M.; Björklund, T.; Lundberg, C.; Kirik, D.; Wandless, T. J., A general chemical method to regulate protein stability in the mammalian central nervous system. *Chem. Biol.* **2010,** *17*, 981-8.
49. Shoulders, M. D.; Ryno, L. M.; Genereux, J. C.; Moresco, J. J.; Tu, P. G.; Wu, C.; Yates, J. R.; Su, A. I.; Kelly, J. W.; Wiseman, R. L., Stress-independent activation of XBP1s and/or ATF6 reveals three functionally diverse ER proteostasis environments. *Cell Rep.* **2013,** *3*, 1279-1292.
50. Chen, J. J.; Genereux, J. C.; Qu, S.; Hulleman, J. D.; Shoulders, M. D.; Wiseman, R. L., ATF6 activation reduces the secretion and extracellular aggregation of destabilized variants of an amyloidogenic protein. *Chem. Biol.* **2014,** *21*, 1564-74.
51. Dewal, M. B.; DiChiara, A. S.; Antonopoulos, A.; Taylor, R. J.; Harmon, C. J.; Haslam, S. M.; Dell, A.; Shoulders, M. D., XBP1s links the unfolded protein response to the molecular architecture of mature N-glycans. *Chem. Biol.* **2015,** *22*, 1301-12.
52. Wong, M. Y.; Chen, K.; Antonopoulos, A.; Kasper, B. T.; Dewal, M. B.; Taylor, R. J.; Whittaker, C. A.; Hein, P. P.; Dell, A.; Genereux, J. C.; Haslam, S. M.; Mahal, L. K.; Shoulders, M. D., XBP1s activation can globally remodel N-glycan structure distribution patterns. *Proc. Natl. Acad. Sci. U. S. A.* **2018,** *115*, E10089-E10098.
53. Wires, E. S.; Henderson, M. J.; Yan, X.; Bäck, S.; Trychta, K. A.; Lutrey, M. H.; Harvey, B. K., Longitudinal monitoring of Gaussia and Nano luciferase activities to concurrently assess ER calcium homeostasis and ER stress in vivo. *PLoS One* **2017,** *12*, e0175481.
54. Kroeger, H.; Grimsey, N.; Paxman, R.; Chiang, W.-C.; Plate, L.; Jones, Y.; Shaw, P. X.; Trejo, J.; Tsang, S. H.; Powers, E.; Kelly, J. W.; Wiseman, R. L.; Lin, J. H., The unfolded protein response regulator ATF6 promotes mesodermal differentiation. *Sci. Signaling* **2018,** *11*, eaan5785.
55. Subramanian, A.; Tamayo, P.; Mootha, V. K.; Mukherjee, S.; Ebert, B. L.; Gillette, M. A.; Paulovich, A.; Pomeroy, S. L.; Golub, T. R.; Lander, E. S. et al. Gene set enrichment analysis: a knowledge-based approach for interpreting genome-wide expression profiles. *Proc. Natl. Acad. Sci. U. S. A.* **2005,** *102*, 15545-15550.
56. Todorova, T.; Bock, F. J.; Chang, P., Poly (ADP-ribose) polymerase-13 and RNA regulation in immunity and cancer. *Trends Mol. Med.* **2015,** *21*, 373-384.

57. Ghimire, D.; Rai, M.; Gaur, R., Novel host restriction factors implicated in HIV-1 replication. *J. Gen. Virol.* **2018,** *99*, 435-446.
58. Zhu, Y.; Chen, G.; Lv, F.; Wang, X.; Ji, X.; Xu, Y.; Sun, J.; Wu, L.; Zheng, Y.-T.; Gao, G., Zinc-finger antiviral protein inhibits HIV-1 infection by selectively targeting multiply spliced viral mRNAs for degradation. *Proc. Natl. Acad. Sci. U. S. A.* **2011,** *108*, 15834-15839.
59. Fujimoto, M.; Takii, R.; Takaki, E.; Katiyar, A.; Nakato, R.; Shirahige, K.; Nakai, A., The HSF1–PARP13–PARP1 complex facilitates DNA repair and promotes mammary tumorigenesis. *Nat. Commun.* **2017,** *8*, 1638.
60. Fujimoto, M.; Takii, R.; Katiyar, A.; Srivastava, P.; Nakai, A., Poly (ADP-ribose) polymerase 1 promotes the human heat shock response by facilitating heat shock transcription factor 1 binding to DNA. *Mol. Cell. Biol.* **2018,** *38*, e00051-18.
61. The ENCODE Project Consortium. Identification and analysis of functional elements in 1% of the human genome by the ENCODE pilot project. *Nature* **2007,** *447*, 799.
62. Gurer, C.; Cimarelli, A.; Luban, J., Specific incorporation of heat shock protein 70 family members into primate lentiviral virions. *J. Virol.* **2002,** *76*, 4666-4670.
63. Franke, E. K.; Yuan, H. E. H.; Luban, J., Specific incorporation of cyclophilin A into HIV-1 virions. *Nature* **1994,** *372*, 359-362.
64. Bartz, S. R.; Pauza, C. D.; Ivanyi, J.; Jindal, S.; Welch, W. J.; Malkovsky, M., An Hsp60 related protein is associated with purified HIV and SIV. *J. Med. Primatol.* **1994,** *23*, 151-154.
65. Matysiak, J.; Lesbats, P.; Mauro, E.; Lapaillerie, D.; Dupuy, J.-W.; Lopez, A. P.; Benleulmi, M. S.; Calmels, C.; Andreola, M.-L.; Ruff, M. et al. Modulation of chromatin structure by the FACT histone chaperone complex regulates HIV-1 integration. *Retrovirology* **2017,** *14*, 39.

For Table of Contents Use Only

HSF1 Activation Can Restrict HIV-1 Replication

Emmanuel E. Nekongo, Anna I. Ponomarenko, Mahender B. Dewal, Vincent L. Butty, Edward P. Browne, Matthew D. Shoulders.

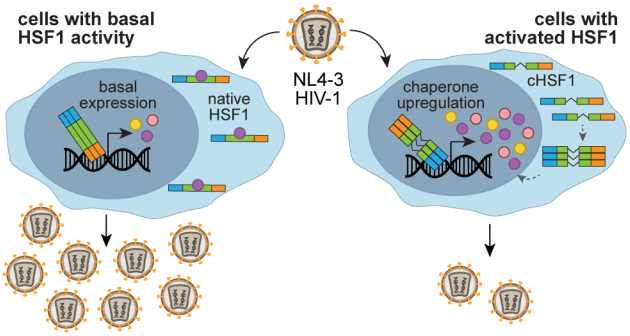

Supporting Information

HSF1 Activation Can Restrict HIV Replication

Emmanuel E. Nekongo, Anna I. Ponomarenko, Mahender B. Dewal, Vincent L. Butty, Edward P. Browne, Matthew D. Shoulders*

Supporting Methods

Plasmids. The following lentiviral destination vectors were used for stable cell line construction: pLenti CMV/TO zeo DEST with either human cHSF1[1] or CFP inserts (Addgene), pLenti6/V5 DEST Gateway with a tetracycline repressor insert (Invitrogen), pLenti CMV puro DEST (Invitrogen) with a DHFR.YFP fusion insert, and previously described DHFR.ATF6(1–373)- and XBP1s-encoding pLenti vectors.[2]

Cell Culture. Human T lymphocytes (CEM) were grown in RPMI-1640 medium (Corning) supplemented with 10% heat-inactivated fetal bovine serum (FBS; CellGro), 1% penicillin/streptomycin/glutamine (CellGro) at 37 °C with 5% CO_2(g). TZM-bl reporter cells were obtained from the NIH AIDS Reagent Program. TZM-bl cells were cultured in DMEM (Corning) supplemented with 10% heat-inactivated fetal bovine serum (Cellgro), 1% penicillin/streptomycin/glutamine (Cellgro) at 37 °C with 5% CO_2(g).

Stable Cell Line Construction. For the CEM^{cHSF1} and CEM^{Ctrl} cell lines construction, CEM cells were transduced first with lentivirus encoding a blasticidin-resistant tetracycline repressor and then with lentiviruses encoding zeocin-resistant cHSF1 or CFP constructs, respectively. Transduction was accomplished by spinoculation with 2 μg/mL polybrene (Sigma-Aldrich) at 1,240 × *g* for 1–1.5 h. Heterostable cell lines expressing the tetracycline repressor and cHSF1 or CFP were then selected using 10 μg/mL blasticidin (Gibco) and 50 μg/mL zeocin (Invitrogen). Single colonies of CEM^{cHSF1} and CEM^{Ctrl} cells were generated from the heterostable population by seeding 30–40 cells in a 96-well plate in 100 μl of RPMI media without antibiotics for 10–14 days. Clonal populations were then selected and expanded in 24-well plates in 500 μL of RPMI containing 10 μg/mL blasticidin and 50 μg/mL zeocin. Cells were grown to confluency and then screened based on functional testing of the cHSF1 construct using RT-PCR for CEM^{cHSF1} cells (described below) and CFP fluorescence for the CEM^{Ctrl} cell line with or without 1 μg/mL doxycycline (dox; Alfa Aesar). CEM^{Ctrl} cell lines were also engineered to express DHFR.YFP by transduction with lentivirus encoding DHFR.YFP (selection using puromycin at 8 μg/mL and single colony selection as above upon visual inspection of 10 μM trimethoprim (TMP; Alfa Aesar)-treated cells). For the CEM^{DAX} cell line construction, CEM cells were transduced first with lentivirus encoding a blasticidin-resistant tetracycline repressor, then with lentiviruses encoding geneticin-resistant hXBP1s and zeocin-resistant DHFR.ATF6, following the protocol described above. Single colonies were selected and expanded in RPMI with 10 μg/mL blasticidin, 500 μg/mL geneticin sulfate (G418, Enzo Life Sciences) and 50 μg/mL zeocin. The cell lines were characterized by CellTiter-Glo viability assay, RT-PCR, and RNA-Seq, as described below.

Quantitative RT-PCR. CEM^{cHSF1} and CEM^{DAX} cells were seeded at a density of 2×10^5 cells/well in a 6-well plate. The cells were treated with 0.1 % DMSO, 1 μg/mL doxycycline, 10 μM TMP, or both (as indicated) for 18 h, 100 μM sodium arsenite (Alfa Aesar) for 2 h for the heat shock activation control, or 10 μg/mL tunicamycin (Sigma-Aldrich) for 6 h for the UPR activation control. Each treatment was performed in biological triplicate. Cellular RNA was extracted using the E.Z.N.A Total RNA Kit (Omega). 1 μg RNA was reverse transcribed into cDNA using the High-Capacity Reverse Transcription kit (Applied Biosystems). The cDNA reaction was then diluted to 80 μL with molecular biology-grade water and 2 μL of each sample was used for RT-PCR with the 2× Sybr Green Reaction Mix (Roche). To assess heat shock response (HSR) activation, primers for human *RPLP2* (housekeeping gene), *HSP90AA1*, *HSPA1A*, *DNAJB1* genes were used (Table S4). To assess unfolded protein response (UPR) activation, primers for human *GAPDH* (housekeeping gene), *BIP*, *SEC24D*, *ERDJ4*, *HYOU1*, *CHOP* were used (Table S4). Transcript levels were first normalized to *RPLP2* levels for HSR activation and to *GAPDH* for UPR activation for every sample, and then normalized for drug-treated versus vehicle-treated cells.

HIV-1 Infection. CEM^{cHSF1} and CEM^{Ctrl} cells were seeded in T75 vented tissue culture flasks (Corning) at a density of 2.5×10^7 cells/flask in 15 mL of RPMI media. The cells were pre-treated with 1 μg/mL dox for 18 h and infected with NL4-3 virus at a multiplicity of infection (MOI) of 0.04, based on the infectious (TZM-bl) viral titers. To remove unbound virions from culture after 12 h of infection, the cells were pelleted at 2,000 × *g*

for 5 min, washed with 25 mL of PBS, and resuspended in 50 mL of RPMI media supplemented with 1 μg/mL dox. After 4 days. the viral supernatant was harvested, clarified at 2,000 × *g* for 5 min to remove cell debris, and stored at –80 °C. The supernatant was titered using p24 and TZM-bl assays. The infectious TZM-bl titers were used to initiate the subsequent serial passaging infection at an MOI of 0.04. For time-course of infection studies, the cells were plated in 24-well plates at density 1.5×10^5 cells/well in 1.5 mL of RPMI media with and without 1 μg/mL doxycycline. After 18 h, the cells were infected with NL4-3 virus at an MOI of 0.05. The infectious supernatant was harvested at 48, 72 and 96 hours post infection and stored at –80 °C prior titering using the p24 assay. CEM^{DAX} cells were seeded at a density of 5×10^5 cells/well in a 24-well plate and pre-treated with 1 μg/mL dox and 10 μM TMP for 18 h. The cells were infected with NL4-3 virus at an MOI of 0.04 as described above and viral supernatant was titered using the p24 assay.

p24 Assay. ELISA plates were prepared by coating 96-well plates with 100 μL/well of 0.02 mg/mL anti-HIV-1 Gag antibody (Aalto Bio Reagents Ltd) in 1 M $NaHCO_3$ (pH 8.5). After 3 h incubation at rt, plates were washed twice with 200 μL of Tris-buffered saline (TBS; VWR) and blocked with 250 μL of 2% milk in TBS overnight at rt. The plates were stored at –20 °C and washed with 1× phosphate-buffered saline (PBS) twice prior to use. Cell-free viral supernatants were assayed for HIV-1 Gag p24 levels by ELISA. Virus was lysed with an effective concentration of 1% Empigen detergent (Sigma) in a 96-well plate for at least 1 h. After 1 h, the lysate was thoroughly mixed and diluted 500–1000 fold with 0.05% Empigen in TBS. p24 standards were prepared by a serial 4-fold dilution of 40 ng/μL recombinant HIV-1 Gag (Aalto Bio Reagents Ltd) in 0.05% Empigen in TBS. The supernatant from uninfected cells was used as a negative control. First, 100 μL of each diluted lysate, p24 standard dilutions, and a negative control were added to ELISA plates in duplicate and incubated for 3 h at rt. Next, the plate was washed twice with TBS, and then 100 μL/well of 1:10,000 diluted mouse monoclonal anti-HIV-1-p24 antibody conjugated to alkaline phosphatase (Aalto Bio Reagents Ltd) was added and incubated for 1 h at rt. The plate was then washed 4× with 200 μL of 0.1% Tween in PBS and twice with Tropix Assay Buffer (Applied Biosystems). Next, the plate was incubated with 50 μL of ([3-(1-chloro-3'-methoxyspiro[adamantane-4,4'-dioxetane]-3'-yl)phenyl] dihydrogen phosphate) (CSPD) substrate with Sapphire II enhancer (Invitrogen) for 30 min. Luminescence was quantified using a Take-3 plate reader (BioTek), monitoring each well for 2 sec.

TZM-bl Assay. TZM-bl reporter cells were seeded at a density of 2.5×10^4 cells/well in 48-well plates. After 5 h, the cells were infected with 100 μL of serially diluted infectious supernatant containing 10 μg/ml polybrene. Each sample was used to infect four technical replicates. After 2 d, the viral supernatant was removed, the cells were washed twice with PBS, and then fixed with 4% paraformaldehyde (Thermo Scientific) for 20 min. After fixing, the cells were washed twice with PBS and stained with 4 mM potassium ferrocyanide, 4 mM ferricyanide, and 0.4 mg/mL 5-bromo-4-chloro-3-indolyl-*p*-D-galactopyranoside (X-Gal) in PBS at 37 °C for 50 min. The cells were washed with PBS, blue cells were counted manually under a microscope, and infectious titers were calculated as the number of blue cells per volume of viral inoculum.

CellTiter-Glo Viability Assay. CEM^{cHSF1} and CEM^{Ctrl} cells were seeded in biological triplicate at a density of 10^3 cells/well in a 96-well plate and pre-treated with 1 μg/mL dox or water (vehicle) for 96 h. The CellTiter-Glo (Promega) assay was then performed according to the manufacturer's instructions. Luminescence was recorded using a Take-3 plate reader (BioTek). The raw fluorescence units for all treatments were normalized to vehicle control.

RNA-Seq. CEM^{HSF1} or CEM^{Ctrl} cells were seeded at a density of 2×10^5 cells/well in a 24-well plate in quadruplicate. The cells were treated with either vehicle or 1 μg/mL dox for 18 h. Cellular RNA was harvested using the RNeasy Plus Mini Kit with QIAshredder homogenization columns (Qiagen). RNA-Seq libraries were prepared using the Kapa mRNA HyperPrep RNA-Seq library construction kit (Kapa/Roche), with 7 min fragmentation at 94 °C and 15 PCR cycles of final amplification and duplex barcoding. Libraries were quantified using the Fragment Analyzer and qPCR before being sequenced on an Illumina HiSeq 2000 using 40-bp single-end reads in High Output mode. Reads were aligned against hg19 (Feb., 2009) using bwa mem v. 0.7.12-r1039 [RRID:SCR_010910] with flags –t 16 –f and mapping rates, fraction of multiply-mapping reads, number of

unique 20-mers at the 5′ end of the reads, insert size distributions and fraction of ribosomal RNAs were calculated using bedtools v. 2.25.0 [RRID:SCR_006646].[3] In addition, each resulting bam file was randomly downsampled to a million reads, which were aligned against hg19 and read density across genomic features were estimated for RNA-Seq-specific quality control metrics. For mapping and quantitation, reads were aligned against GRCh38/ENSEMBL 89 annotation using STAR v. 2.5.3a with the following flags -runThreadN 8 –runMode alignReads –outFilter-Type BySJout –outFilterMultimapNmax 20 –alignSJoverhangMin 8 –alignSJDBoverhangMin 1 –outFilterMismatchNmax 999 –alignIntronMin 10 –alignIntronMax 1000000 –alignMatesGapMax1000000 –outSAMtype BAM SortedByCoordinate –quantMode TranscriptomeSAM with –genomeDir ointing to a 75nt-junction GRCh38 STAR suffix array.[4] Gene expression was quantitated using RSEM v. 1.3.0 [RRID:SCR_013027] with the following flags for all libraries: rsem-calculate-expression –calc-pme –alignments -p 8 –forward-prob 0 against an annotation matching the STAR SA reference.[5] Posterior mean estimates (pme) of counts and estimated RPKM were retrieved. For differential expression analysis, dox-treated CEM-^{cHSF1} cells were compared against vehicle-treated CEM^{cHSF1} samples. Briefly, differential expression was analyzed in the R statistical environment (R v.3.4.0) using Bioconductor's DESeq2 package on the protein-coding genes only [RRID:SCR_000154].[6] Dataset parameters were estimated using the estimateSizeFactors(), and estimateDispersions() functions; read counts across conditions were modeled based on a negative binomial distribution, and a Wald test was used to test for differential expression (nbinomWaldtest(), all packaged into the DESeq() function), using the treatment type as a contrast. Shrunken log2 fold-changes were calculated using the lfcShrink function. Fold-changes and p-values were reported for each protein-coding gene. Gene ontology analyses were performed using the online DAVID server.[7] Heat maps for select genes were generated in GraphPad Prism version 7.0b (Figure S2).

Gene Set Enrichment Analysis (GSEA). Differential expression results from DESeq2 were retrieved, and the "stat" column was used to pre-rank genes for GSEA analysis. Briefly, this "stat" values reflects the Wald's test performed on read counts as modeled by DESeq2 using the negative binomial distribution. Genes that were not expressed were excluded from the analysis. Alternatively, gene loadings from PCA analysis were used as ranking metrics. GSEA (desktop version, v3.0)[8-9] was run in the pre-ranked mode against MSigDB 7.0 Hallmark, C2 (curated gene sets), C5 (Gene Ontology), C6 (oncogenic signatures) and C7 (immunologic signatures) sets, using the official gene symbol as the key, with a weighted scoring scheme, normalizing by meandiv, with gene sets between 5 and 2000 genes (5379 gene sets retained for C2, 830 for C3, 9373 for C5, 189 for C6 and 4872 for C7), and 5000 permutations were run for *p*-value estimation. GSEA enrichment plots were replotted using a modified version of the ReplotGSEA.R script (https://github.com/PeeperLab/Rtoolbox/blob/master/R/ReplotGSEA.R).

Statistical Analyses. All experiments were performed in biological triplicate with the data presented as mean ± standard deviation. Statistical significance was assessed using unpaired *t*-tests with Welch's correction in GraphPad Prism version 7.0b.

Supporting References

1. Shoulders, M. D.; Ryno, L. M.; Cooley, C. B.; Kelly, J. W.; Wiseman, R. L., Broadly applicable methodology for the rapid and dosable small molecule-mediated regulation of transcription factors in human cells. *J. Am. Chem. Soc.* **2013,** *135*, 8129-8132.
2. Shoulders, M. D.; Ryno, L. M.; Genereux, J. C.; Moresco, J. J.; Tu, P. G.; Wu, C.; Yates, J. R.; Su, A. I.; Kelly, J. W.; Wiseman, R. L., Stress-independent activation of XBP1s and/or ATF6 reveals three functionally diverse ER proteostasis environments. *Cell Rep.* **2013,** *3*, 1279-1292.
3. Quinlan, A. R.; Hall, I. M., BEDTools: A flexible suite of utilities for comparing genomic features. *Bioinformatics* **2010,** *26*, 841-842.
4. Dobin, A.; Davis, C. A.; Schlesinger, F.; Drenkow, J.; Zaleski, C.; Jha, S.; Batut, P.; Chaisson, M.; Gingeras, T. R., STAR: ultrafast universal RNA-seq aligner. *Bioinformatics* **2013,** *29*, 15-21.
5. Li, B.; Dewey, C. N., RSEM: accurate transcript quantification from RNA-Seq data with or without a reference genome. *BMC Bioinform.* **2011,** *12*, 323.
6. Love, M. I.; Huber, W.; Anders, S., Moderated estimation of fold change and dispersion for RNA-seq data with DESeq2. *Genome Biol.* **2014,** *15*, 550.
7. Huang, D. W.; Sherman, B. T.; Lempicki, R. A., Bioinformatics enrichment tools: paths toward the comprehensive functional analysis of large gene lists. *Nucleic Acids Res.* **2008,** *37*, 1-13.
8. Mootha, V. K.; Lindgren, C. M.; Eriksson, K.-F.; Subramanian, A.; Sihag, S.; Lehar, J.; Puigserver, P.; Carlsson, E.; Ridderstråle, M.; Laurila, E., PGC-1α-responsive genes involved in oxidative phosphorylation are coordinately downregulated in human diabetes. *Nat. Genet.* **2003,** *34*, 267.
9. Subramanian, A.; Tamayo, P.; Mootha, V. K.; Mukherjee, S.; Ebert, B. L.; Gillette, M. A.; Paulovich, A.; Pomeroy, S. L.; Golub, T. R.; Lander, E. S., Gene set enrichment analysis: A knowledge-based approach for interpreting genome-wide expression profiles. *Proc. Natl. Acad. Sci. U.S.A.* **2005,** *102*, 15545-15550.

Supporting Figures

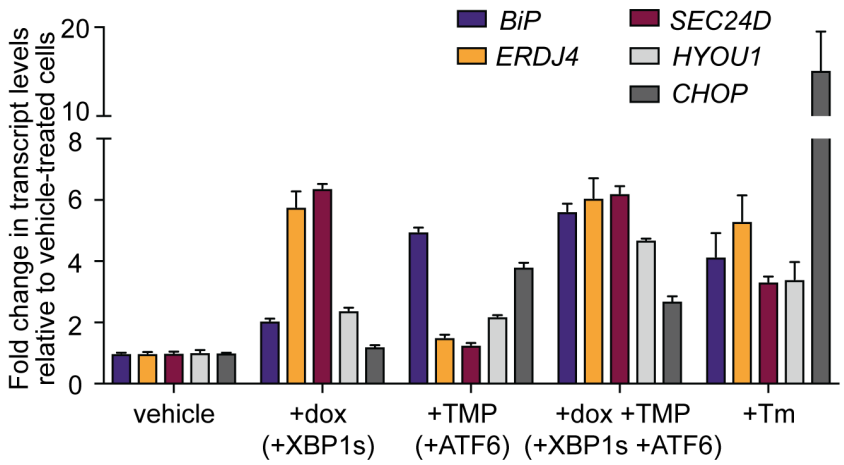

Figure S1. Selective induction of XBP1s and/or ATF6 target genes in CEM^{DAX} cells. qPCR analysis of the unfolded protein response genes (*BiP*, *ERDJ4*, *SEC24D*, *HYOU1*, *CHOP*) expression levels upon tet-XBP1s activation with 1 μg/mL doxycycline for 18 h, DHFR-ATF6 activation with 10 μM trimethoprim for 18 h, or both, and 10 μg/mL tunicamycin (Tm) treatment as a positive control for stress-mediated unfolded protein response activation.

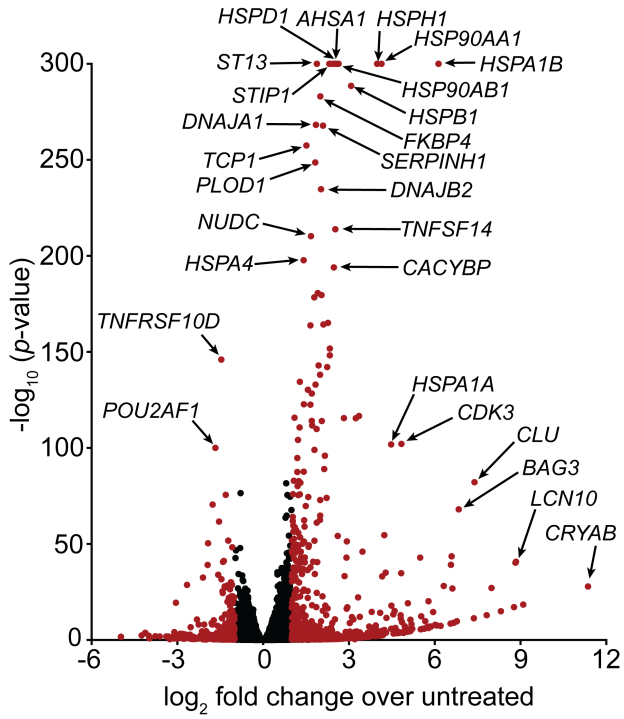

Figure S2. Transcriptional profile of HSF1-activated host environment. Volcano plot showing distribution of expressed transcripts upon HSF1 activation with 1 μg/mL doxycycline for 18 h in CEM^{cHSF1} cells. Red dots correspond to transcripts displaying ≥ 2-fold expression changes with p-values ≤ 10^{-5}. Genes with *p*-value of 0 were assigned an absolute maximum *p*-value of 10^{-300} for the purpose of display on the volcano plot.

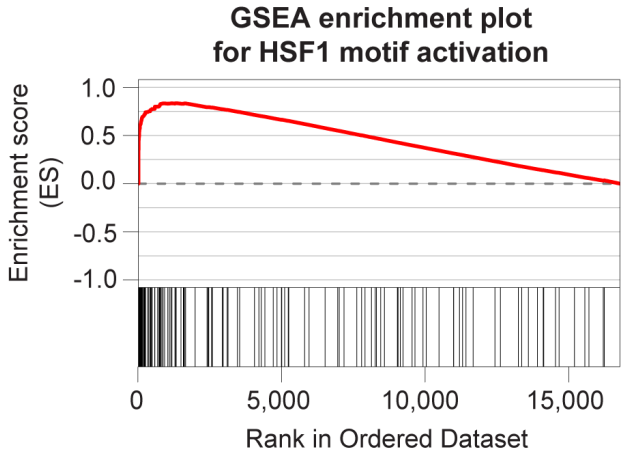

Figure S3. Heat shock factor (HSF) motif is enriched upon cHSF1 induction with 1 µg/mL doxycycline for 18 h in CEM^{cHSF1} cells. Gene set enrichment plot of HSF motif using TTCNRGNNNNTTC_HSF_Q6 gene set from MSigDB c3 collection.

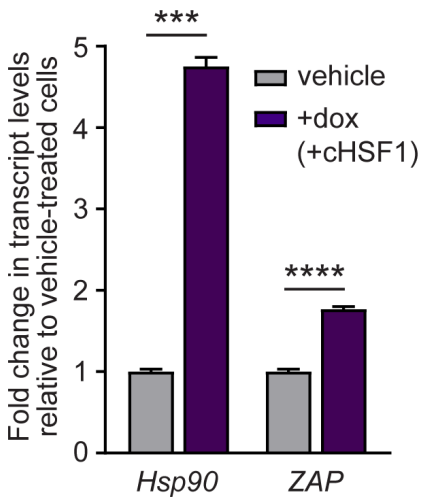

Figure S4. Induction of cHSF1 activates ZAP transcription. qPCR analysis of the classical heat shock response gene Hsp90 and ZAP expression levels upon treatment of CEM^{cHSF1} cells with 1 μg/mL doxycycline for 18 h. *** and ****correspond to *p*-values <0.001 and <0.0001, respectively.

Supporting Tables

Table S1. RNA-Seq characterization of CEM^{cHSF1} cells: Differential expression analysis of HSF1-activated environment.

Table S2. RNA-Seq characterization of CEM^{cHSF1} cells: Gene set enrichment analysis.
Table S2A (Sheet 1): GSEA results of upregulated genes for cHSF1 activation using MSigDB c5.
Table S2B (Sheet 2): GSEA results of downregulated genes for cHSF1 activation using MSigDB c5.
Table S2C (Sheet 3): GSEA results of upregulated genes for cHSF1 activation using MSigDB c3.
Table S2D (Sheet 4): GSEA results of upregulated genes for cHSF1 activation using MSigDB c2.
Table S2E (Sheet 5): GSEA results of downregulated genes for cHSF1 activation using MSigDB c2.

Table S3. Gene list for the 'Defense Response to Virus' gene ontology group showing enrichment scores upon cHSF1 induction.

Table S4. Sequences of RT-PCR primers used.

Gene	Forward primer sequence	Reverse primer sequence
RPLP2	CGTCGCCTCCTACCTGCT	CCATTCAGCTCACTGATAACCTT
HSP90AA1	GATAAACCCTGACCATTCC	AAGACAGGAGCGCAGTTTCATAAA
HSPA1A	GGAGGCGGAGAAGTACA	GCTGATGATGGGGTTACA
DNAJB1	TGTGTGGCTGCACAGTGAAC	ACGTTTCTCGGGTGTTTTGG
GAPDH	TGGAAGGACTCATGACCACA	AGGGGTCTACATGGCAACTG
BIP	GCCTGTATTTCTAGACCTGCC	TTCATCTTGCCAGCCAGTTG
ERDJ4	CTGTATGCTGATTGGTAGAGTCAA	AGTAGACAAAGGCATCATTTCCAA
SEC24D	AGCAGACTGTCCTGGGAAGC	TTTGTTTGGGGCTGGAAAAG
HYOU1	GCAGACCTGTTGGCACTGAG	TCACGATCACCGGTGTTTTC
CHOP	GGAGCTGGAAGCCTGGTATG	GCCAGAGAAGCAGGGTCAAG
ZAP	GCACTTGTTAACGATTCTTTATCTG	AGCGGACAACCCTTACACAG